

# Preparation of Coal-Based Graphene by Flash Joule Heating

Xinjuan Liu and Hongchao Luo\*

Cite This: *ACS Omega* 2024, 9, 2657–2663

Read Online

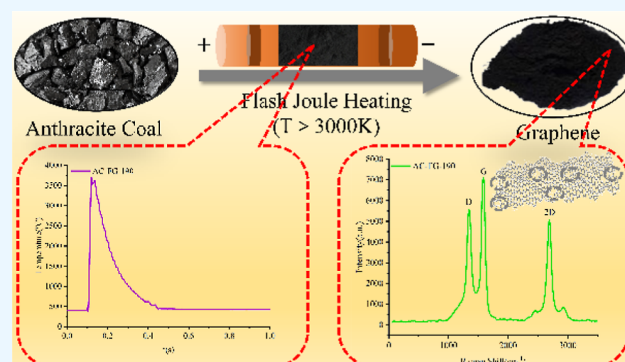
ACCESS |

Metrics &amp; More

Article Recommendations

Supporting Information

**ABSTRACT:** This study explores the production of flash graphene (AC-FG) from anthracite coal by using the flash Joule heating (FJH) method. This study demonstrates that AC-FG can be derived from anthracite coal by precisely controlling the system parameters, specifically the pulse voltage. The FJH process requires no catalyst. The produced material was characterized by using Raman, XRD, XPS, TG, SEM, TEM, and XPS techniques. The results reveal that the degree of graphitization of coal reaches its peak at 190 V. From an energy perspective, FJH provides a straightforward and cost-effective method for graphene preparation, offering a substantial avenue for the efficient utilization of coal resources and the cost-effective application of graphene.



## 1. INTRODUCTION

Graphene, a novel material composed of  $sp^2$ -hybridized carbon atoms forming a tightly packed monolayer in a two-dimensional honeycomb lattice, exhibits a considerable specific surface area and unique electronic properties, high mobility, and excellent transport characteristics.<sup>1</sup> These attributes render it highly promising across diverse fields such as materials science, energy, biomedicine, drug delivery, and catalysis, positioning it as a revolutionary material of the future.<sup>2–7</sup> Presently, graphene synthesis methods fall into two categories: top-down exfoliation of the top layer and bottom-up growth from the base layer.<sup>8</sup> Top-down methods employ various physical and chemical processes to weaken the van der Waals forces between graphite layers and achieve single- or few-layer graphenes. Mechanical exfoliation,<sup>9</sup> liquid-phase exfoliation,<sup>10</sup> redox exfoliation,<sup>11</sup> electrochemical exfoliation,<sup>12</sup> and microwave exfoliation are the primary techniques.<sup>13,14</sup> Conversely, bottom-up approaches involve chemical reactions of precursors to produce controlled, large-area single-layer graphene,<sup>15</sup> mainly through chemical vapor deposition<sup>16</sup> and epitaxial growth.<sup>17</sup> These techniques each exhibit drawbacks, limiting their scalability for graphene production. Consequently, a need persists for a rapid, simple, cost-effective, and scalable production process.<sup>18</sup>

Flash Joule heating (FJH) was first introduced by Luong et al. in a 2020 Nature publication. This process converts carbon-containing feedstocks, including carbon black, waste plastics, rubber tires, coal, and coal pitch, into high-quality turbo graphene (tFG).<sup>19</sup> FJH stands as a mass-producible and efficient graphene production method that circumvents the necessity for solvents, catalysts, or inert gases. The cost for transforming 1 ton of amorphous carbon to graphene through FJH ranges from \$30 to \$161.<sup>20</sup> tFG exhibits superior oxidative

stability compared to that of the graphene oxide synthesized through traditional methods.<sup>21</sup> With China's "rich in coal, poor in oil, and low in gas" reality, diversifying the application of coal, an abundantly available and affordable carbon-rich mineral resource, becomes imperative.<sup>22</sup> Coal composition and properties vary by type, with multiple coal grades such as anthracite, charcoal, metallurgical coke, and coal pitch successfully converted into FG.<sup>23</sup> Numerous studies have shown that the structure and composition of carbon materials are highly dependent on their heat treatment temperature, heating/cooling rate, duration, and environment.<sup>24</sup>

This study involves preparing coal-based graphene using the FJH method, harnessing in situ heat generated from the sample's resistance and capacitor assembly discharge. This process generates momentary high temperatures exceeding 3000 K on the millisecond scale, facilitating coal-based graphene synthesis conditions. This study analyzes the products' structure, morphology, elemental content, and stability through various characterization techniques while also investigating the impact of flashing voltage on the products.

## 2. EXPERIMENTAL SECTION

**2.1. Materials.** The main materials and reagents included anthracite coal (AC) from Guizhou Province, China,

Received: September 29, 2023

Revised: December 2, 2023

Accepted: December 21, 2023

Published: January 4, 2024



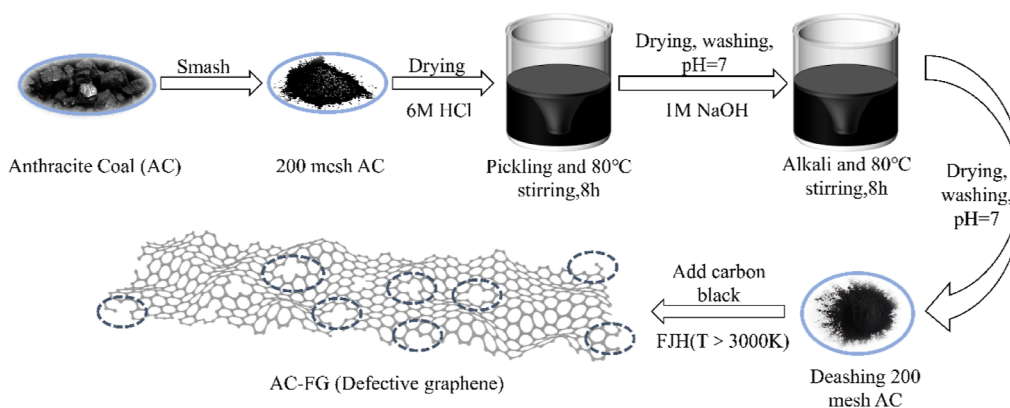


**Figure 1.** Schematic illustration of the preparation of AC-FG from Guizhou anthracite by FJH.

**Table 1.** Proximate and Ultimate Analyses of Puan Anthracite<sup>a</sup>

sample analysis	proximate analysis (wt %)				ultimate analyses (wt %, daf)				
	M <sub>ad</sub>	A <sub>d</sub>	V <sub>daf</sub>	FC <sub>daf</sub>	C	H	O	N	S
AC	1.19	29.92	11.67	57.22	60.68	4.96	5.01	1.16	3.01
t-AC	0.85	24.45	10.16	64.54	65.80	4.52	3.92	1.14	2.56

<sup>a</sup>M<sub>ad</sub>: air-dry base moisture; A<sub>d</sub>: dry base ash; V<sub>daf</sub>: dry ash-free volatiles; and FC<sub>daf</sub>: dry ash-free fixed carbon.

anhydrous ethanol (AR), hydrochloric acid (AR), sodium hydroxide (AR), and carbon black (AR).

**2.2. Flash Joule Heating Experiment.** Two models of the Sai Yin pulse electro-flash reactor were available: FJH-2023A and FJH-2023B. The FJH-2023A model, developed by Shanxi University, was primarily used in this experiment, as shown in Figure S1. Figure 1 depicts the entire preparation process of flash coal-based graphene (AC-FG). In general, AC-FG with a layered structure is synthesized after grinding, drying, acid and alkali deashing, deionized water washing and FJH.

**2.2.1. Preprocessing.** The raw coal was dried overnight in a vacuum at 80 °C before flashing. The AC was crushed into a 200-mesh (0.074 mm) powder using a grinder (high-speed multifunctional crusher-800Y, Huang Cheng).

Due to the presence of numerous inorganic mineral components in coal, which exist in a complex state, it exerts an adverse influence on the generation of the final product.<sup>25</sup> In order to mitigate the impact of mineral components in Puan anthracite on the product of coal-based graphene, the coal sample was pretreated for deashing. The Raman spectrum of the product obtained from anthracite without pretreatment after being treated with FJH is shown in Figure S2. The figure shows that no 2D characteristic peak of coal-based graphene is found. Therefore, it is considered whether the formation of noncoal-based graphene is caused by the high ash content in coal. According to the reported literature, the commonly used ash removal methods are the hydrofluoric acid method, conventional acid–base method, molten alkali leaching method, solvent extraction method, heavy medium separation method, microwave pretreatment method, and oil-screening method.<sup>26</sup> Among them, the conventional acid–base method can remove toxic and harmful elements (lead, mercury, arsenic, cadmium, germanium, etc.) and pyrite ore in coal under normal temperature and pressure conditions, and the reaction technology is mature and the process is adaptable. Among these methods, the NaOH–HCl method is the most commonly used.<sup>27</sup>

The AC powder underwent pretreatment with 6 M HCl and 1 M NaOH. The primary chemical reactions involved in the combined NaOH–HCl deashing process are shown in eqs 1–6.<sup>28</sup> The sample was washed with deionized water until the pH reached 7 and then dried at 80 °C for 8 h. The resulting product was deashed coal, referred to as t-AC.

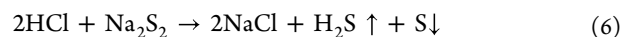
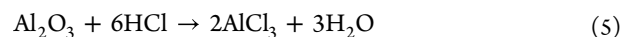
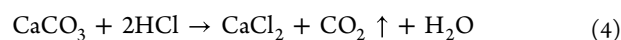
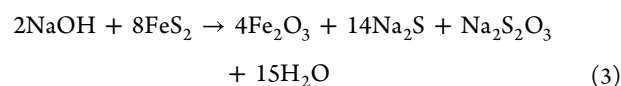
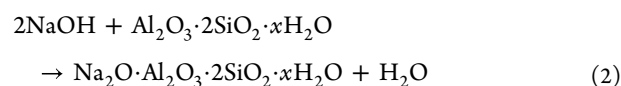
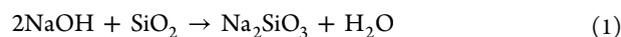
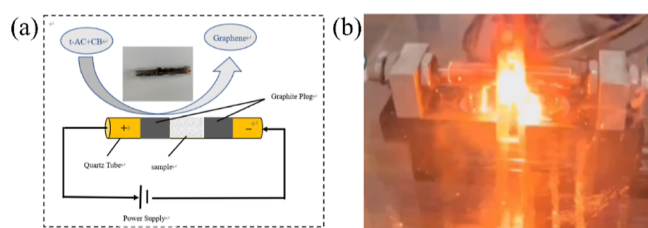


Table 1 shows the proximate and ultimate analyses of Puan anthracite data before and after sample deashing. After the deashing treatment, the ash content decreased from the initial value of 29.92 to 24.45%, and the ash removal rate was 18.3%, which has a certain removal effect on minerals. The mass fraction of sulfur in the coal samples changed little before and after desliming, indicating that the sulfur content in the coal samples mainly existed in the form of organic sulfur.<sup>29</sup>

**2.2.2. Flash Joule Heating Experiment.** Due to the high resistance of t-AC, a conductive material is needed to be added to ensure experimental feasibility. In this case, conductive carbon black was introduced. Notably, graphene was not generated without the addition of conductive carbon black. Adding 20 mg of carbon black decreased the resistance of the carbon black t-AC mixture from 280 to less than 100 Ω. In the FJH system (Figure 2a), adjusting the pulse voltage and time led to variations in the peak current and total energy within the sample, thereby influencing the peak temperature and time



**Figure 2.** (a) Simplified scheme of the FJH setup (a detailed diagram of the device is shown in Figure S1) and the (b) moment when a spark occurs during the flash-voltage process.

needed to reach that peak temperature.<sup>30</sup> Bright sparks appear when high temperatures are generated (Figure 2b). In this study, the mixture underwent treatment using the FJH system with the same discharge time (0.5 s) but different flash voltages (100, 130, 150, 170, and 190 V), resulting in products designated AC-FG-100, AC-FG-130, AC-FG-150, AC-FG-170, and AC-FG-190, respectively. It is worth noting that before the reaction, the reaction device needs to be vacuumed, and the sample is pretreated with a voltage of 30–50 V to prevent excessive voltage spatter, resulting in reduced product recovery. The FJH setup employed in this experiment featured a capacitance of 90 mF, a voltage range of 0–300 V, a quartz tube diameter of  $d = 8$  mm, and a length of  $l = 70$  mm.

**2.3. Material Characterization.** Raman measurements of the products were performed using a Raman spectrometer (Horiba LabRAM HR Evolution, Japan) equipped with a 532 nm laser line to analyze the chemical composition and structure of AC-FG. Scans were conducted in the 50 to 4000  $\text{cm}^{-1}$  range. X-ray powder diffraction was executed using a Rigaku SmartLab SE diffractometer from Japan utilizing a  $\text{Cu K}\alpha$  ( $\lambda = 0.154178$  nm) radiation source. Data collection occurred within the 5–80° range at a scan rate of 5°/min, elucidating the phase structure of AC-FG. The morphology and microstructure of AC-FG were investigated by scanning electron microscopy (Zeiss GeminiSEM 300, Germany) and transmission electron microscopy (JEOL JEM-F200, Japan). Given the limited observation range of HR-TEM images, multiple experiments were conducted from different points to ensure a comprehensive representation, and the most representative images were ultimately selected. Fourier transform and inverse Fourier transform analyses were applied to TEM images, preserving the original structural information and enhancing the image clarity. The elemental distribution of the products was assessed using XPS (Thermo Scientific K-Alpha, USA), with all XPS spectra referenced against the C 1s peak

(284.5 eV). The stability of the products under different flash voltages was characterized using a TA Discovery TGA 550 thermogravimetric analyzer from the USA. Data collection spanned 50–900 °C with a ramp rate of 10 °C/min ( $\text{N}_2$  atmosphere and air atmosphere, respectively).

### 3. RESULTS AND DISCUSSION

**3.1. Flash Joule Heating Experiment Results.** Figure 3 explains why FJH can produce AC-FG. As shown in Figure 3a, the capacitor bank discharge produces Joule heat, rapidly elevating the feedstock's temperature to approximately 2000–3800 °C within a few hundred milliseconds, followed by swift cooling to room temperature within seconds. The peak current also varied based on flash-voltage adjustments, with an approximately 100 ms pulsed current observed during discharge, aligning with the heating curve. The peak current escalated rapidly with an increasing flash voltage (Figure 3b).

**3.2. Morphological and Structural Characterization Results.** The physicochemical properties and microstructure of the materials were characterized by XRD, Raman spectroscopy, SEM, TEM, TGA, and XPS. The results are presented and discussed in the following sections.

Figure 4a–f presents the SEM local magnification images captured by t-AC, AC-FG-100, AC-FG-130, AC-FG-150, AC-FG-170, and AC-FG-190, respectively, while scanning electron micrographs reveal a visible microstructural evolution from low to high crystallinity. SEM full images of the samples before and after the FJH treatment are shown in Figure S3a–f. The observations revealed that t-AC consists of nonuniform amorphous carbon particles, and following FJH, a portion of the amorphous carbon on the sample surface underwent transformation into graphite nanoflakes, exhibiting a tightly stacked lamellar structure of graphene layers.

In the HR-TEM images, as shown in Figure 5a–e, lattice edges belonging to graphene can be clearly observed, and the stacking properties of multiple layers of graphene are shown. The HR-TEM images at other scales are shown in Figure S4a–e. After calculation, it is found that the lattice spacing of AC-FG-190 is 0.358 nm, which is significantly larger than 0.3354 nm of AB-stack graphite,<sup>31</sup> which indicates that turbo-layered graphene is generated by FJH, and the large layer spacing makes it easier to peel between the graphite sheets to form the graphene sheet structure.<sup>32</sup>

From the XRD plot in Figure 6a, it can be observed that following the flash process, the diffraction angle of the (002) plane of AC-FG is approximately 26.0°, calculated according to the formula  $d_{002} = \lambda / (2 \sin \theta_{(002)})$  (where  $\lambda$  is the X-ray

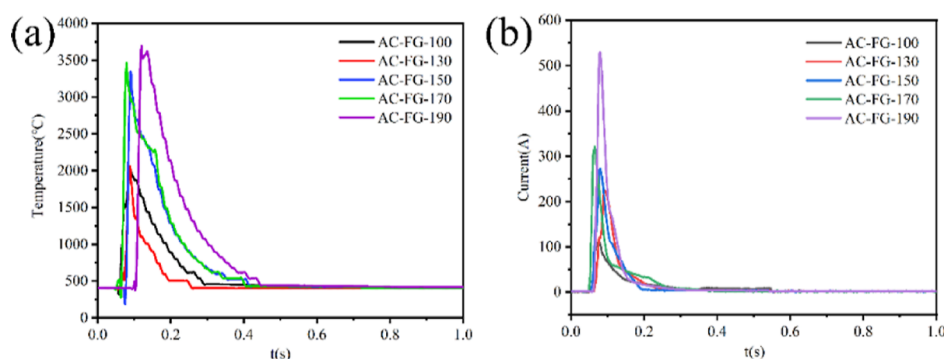


**Figure 3.** (a) Plot of discharge time versus temperature ( $t$ – $T$ ) and (b) plot of discharge time versus current ( $t$ – $I$ ).

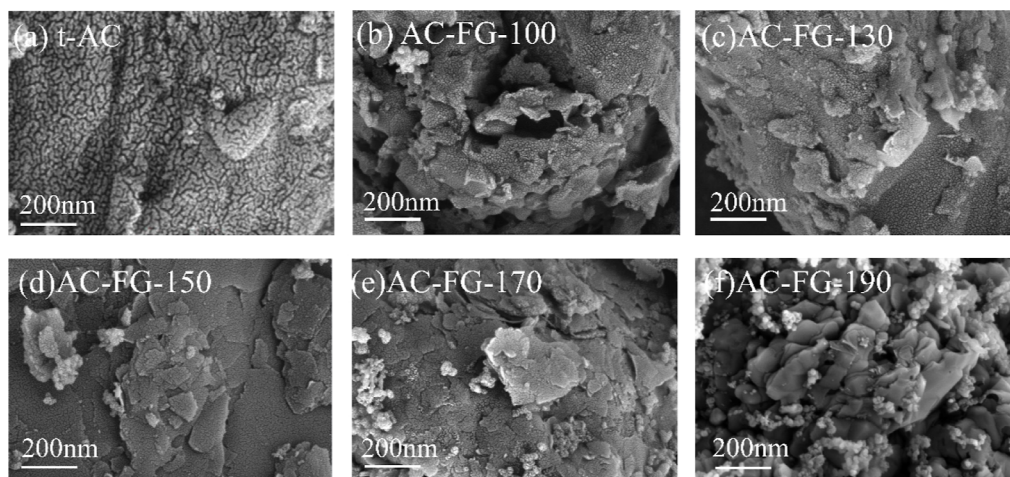


**Figure 4.** (a–f) SEM images of deashing coal and products with different flash voltages (the image scale is 200 nm).

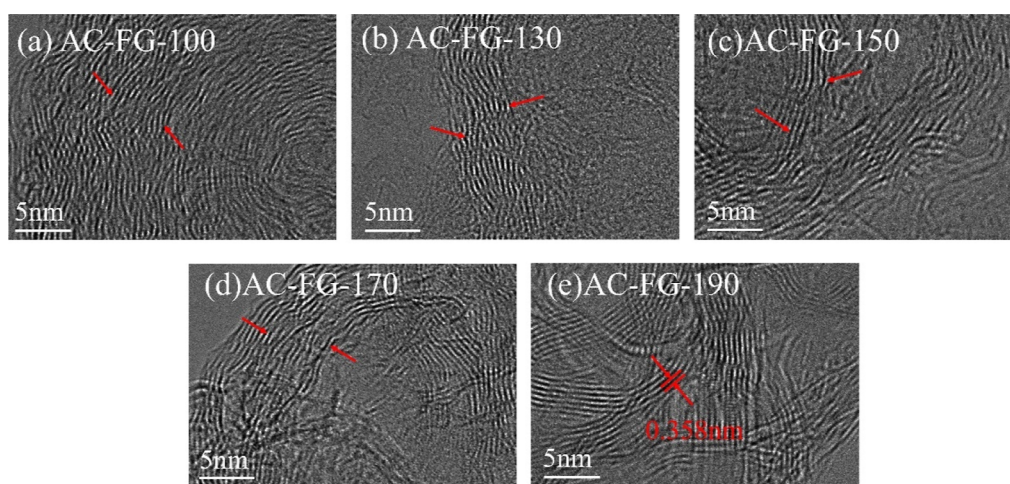


**Figure 5.** (a–e) HR-TEM images of the products treated with different flash voltages on a scale of 5 nm (the graphene sheet structure is marked by arrows).

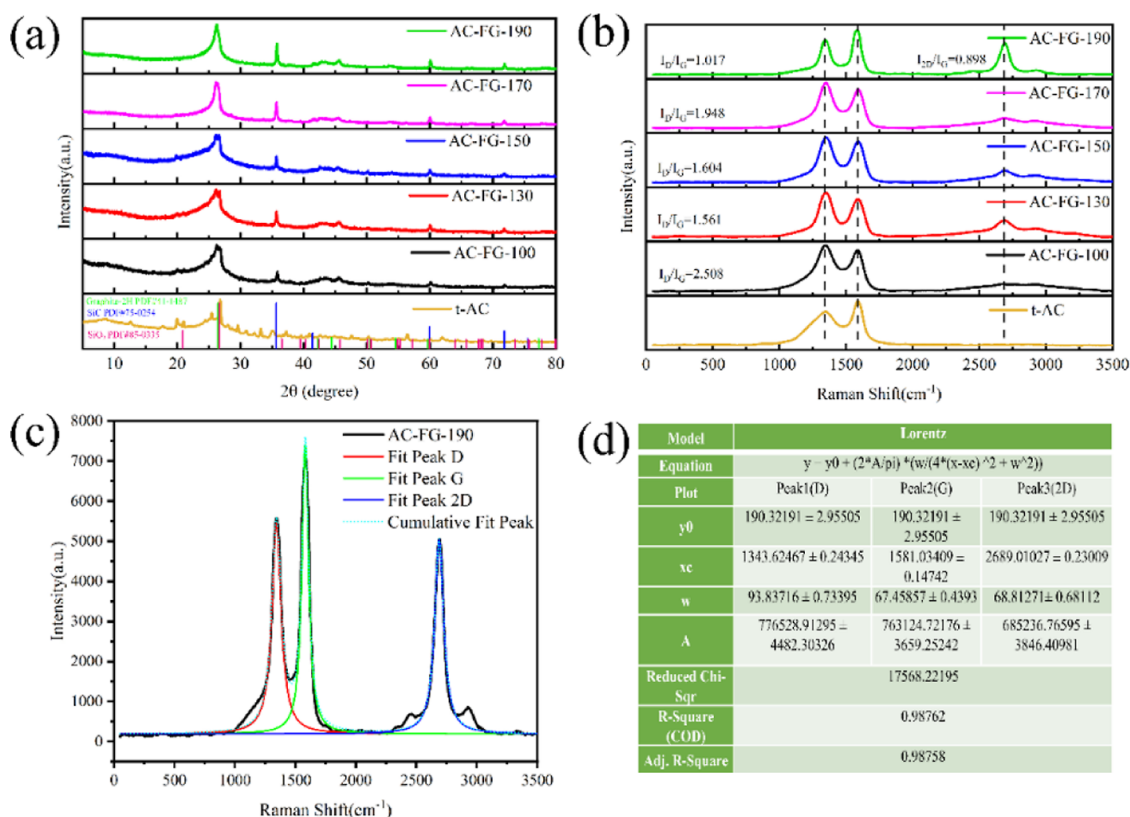
wavelength,  $d_{002}$  is the average layer spacing, and  $\theta$  is the diffraction angle),<sup>33</sup> the interlayer distance of the sample is much greater than 0.334 nm for AB-stack graphite, and combined with the lattice distance of the sample, it is inferred that the product should be turbo-layered graphene.

Furthermore, a higher flashing voltage corresponds to a more pronounced intensity of the (002) plane diffraction peak. This intensity trend suggests that samples subjected to high-voltage flashing exhibit a more regular graphitic microcrystalline structure. Alongside the distinctive peak at approximately  $26.0^\circ$ , stronger SiC diffraction peaks emerge at  $2\theta = 35.7, 59.9,$  and  $72.0^\circ$ . These angles correspond to the cubic crystal  $\beta$ -SiC (111), (200), and (311) crystallographic planes, respectively.<sup>34</sup> The XRD spectra of AC-FG-100, AC-FG-130, and AC-FG-150 V also indicate the presence of weaker characteristic peaks at  $2\theta = 26.6^\circ$ , which correspond to the (111) crystallographic plane of  $\beta$ -SiO<sub>2</sub>. The appearance of SiO<sub>2</sub> diffraction peaks might be attributed to inadequate pretreatment of the impurities in coal. Similarly, the presence of SiC diffraction peaks could be attributed to the reaction between carbon and SiO<sub>2</sub> at high temperatures under a vacuum or an inert atmosphere.<sup>35</sup>

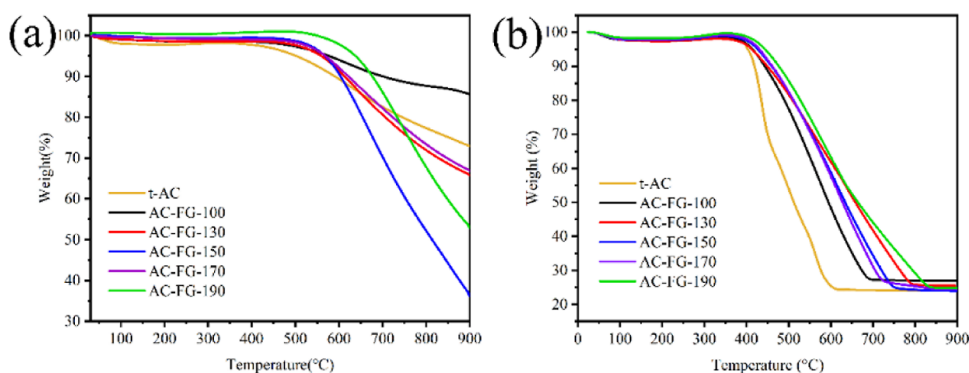
The Raman spectra of graphite samples obtained through heat treatment under various flash conditions are depicted in

Figure 6b. All coal-based graphitized samples exhibit a strong defective D-peak at approximately  $1350\text{ cm}^{-1}$ , attributed to the disordered carbon within the samples, which implies a high presence of material defects. A prominent G-peak at approximately  $1580\text{ cm}^{-1}$  is linked to highly ordered graphite.<sup>36,37</sup> The  $I_D/I_G$  ratio in the Raman spectra, often utilized to gauge the degree of order in microcrystalline graphitic structures, indicates a higher degree of disorder in the product as the  $I_D/I_G$  value increases.<sup>38</sup> Notably, of all the graphitized samples, only AC-FG-190 exhibited a distinct 2D peak at approximately  $2700\text{ cm}^{-1}$ , indicating graphene production and had the lowest  $I_D/I_G = 1.017$ , signifying the highest level of order in its graphitic microcrystalline structure. The  $I_{2D}/I_G$  intensity ratio in Raman spectra is commonly employed to reflect the mass and number of layers of graphene, where  $I_{2D}/I_G < 1$  denotes multilayer graphene and  $I_{2D}/I_G > 1$  signifies monolayer graphene. It can be observed from the figure that varying the pulse voltage within the range of 100–190 V leads to different degrees of graphene mass and conversion due to peak current variations. Lower voltages result in decreased conversion rates, leaving a considerable amount of amorphous carbon after FJH.

According to the literature reported by Beckham et al.,<sup>39</sup> the graphene yield (GY) index prepared using FJH can be



**Figure 6.** (a) XRD spectrum of AC-FG; (b) Raman spectrum of AC-FG; and (c,d) Lorentz-fitted AC-FG-190 Raman spectra.



**Figure 7.** (a) TGA ( $N_2$ ,  $10\text{ }^\circ\text{C}/\text{min}$ ) of the samples before and after the FJH treatment and (b) TGA (air,  $10\text{ }^\circ\text{C}/\text{min}$ ) of the samples before and after the FJH treatment.

determined by dividing the total number of Raman spectra classified as graphene by the total number of Raman spectra in the sample. The discrimination between “graphene” Raman spectra and “amorphous carbon” Raman spectra is based on the full width at half-maximum (fwhm) of  $I_{2D}/I_G$  ( $I_{2D}/I_G > 0.3$ ) and the 2D band ( $15 < \text{fwhm}_{2D} < 70\text{ cm}^{-1}$ ). In Figure 6c,d, the Raman spectrum of AC-FG-190 is fitted using Lorentz, and the data in the table indicate that t-AC undergoes transformation from amorphous carbon to graphene at a flash voltage of 190 V, resulting in a graphene yield of 44%. The Raman spectrum from 100–170 V was fitted using Lorentz (Figure S5), revealing that it did not originate from graphene.

Thermogravimetric analysis (TGA) results (Figure 7) can ascertain the stability of AC-FG in the temperature range from 50 to  $900\text{ }^\circ\text{C}$ . From the figure, we can see that the thermal stability of the flash product is higher than that of the deashing

coal (t-AC), either in an air or in a  $N_2$  atmosphere. As depicted in the figure, all AC-FG samples maintain stability until approximately  $550\text{ }^\circ\text{C}$  in a  $N_2$  atmosphere. The high thermal stability is indicative of the high degree of crystallinity and low defects of the tFG structure as defects often lower the thermal stability of graphene.<sup>40</sup>

The full spectrum of the product is illustrated in Figure 8, highlighting a decrease in elemental oxygen content and an increase in carbon content after flashing at  $\sim 170\text{ V}$ . The results demonstrate that as the flash voltage increases, the C/O in the product progressively rises. This signifies an enhancement in the purity of element C during the FJH process, and higher flash voltages are conducive to the production of coal-based graphite. The C 1s spectrum in Figure S6 exhibits a notable C–C/C=C peak at  $284.5\text{ eV}$ , which is the high-resolution carbon XPS. XPS peaks of slight C–O/C–O–C and O–C=

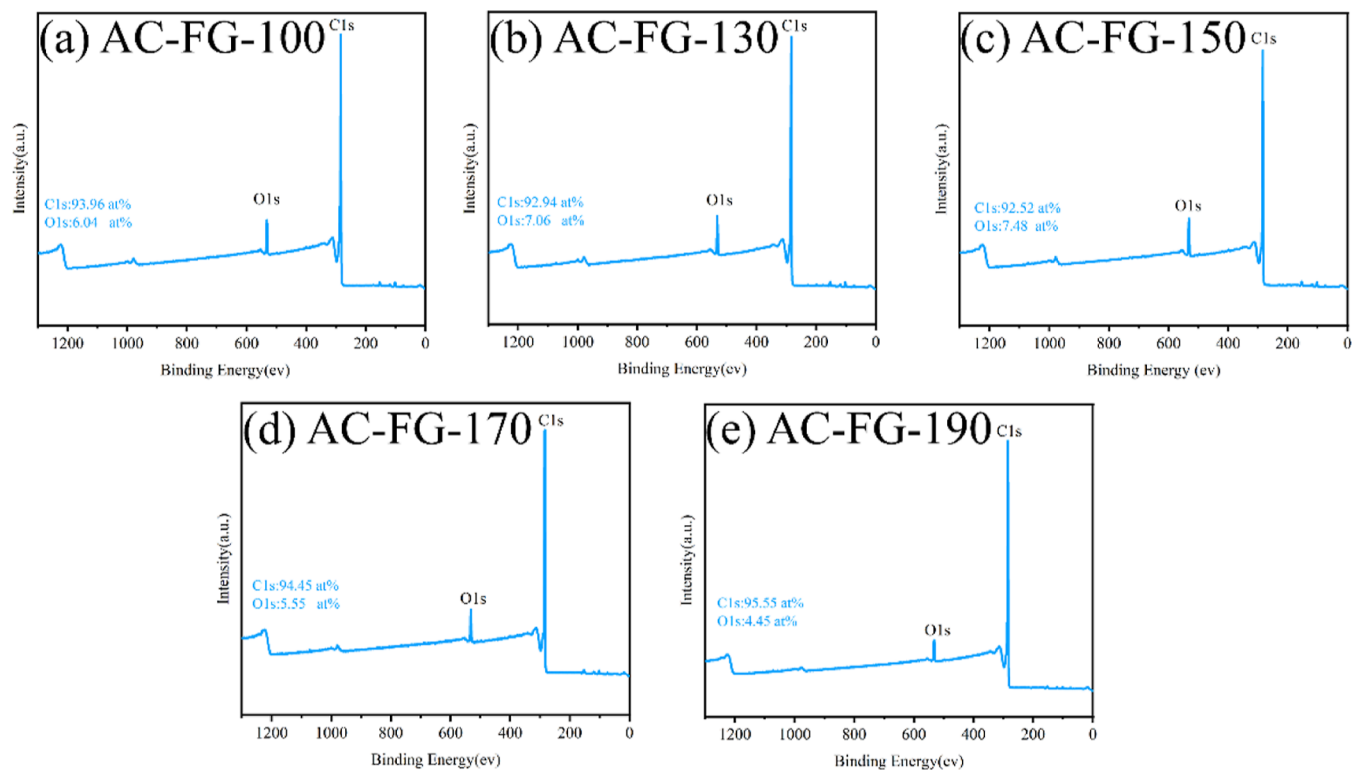


**Figure 8.** (a–e) XPS full spectrum of AC-FG treated with different flash voltages.

O spectra were observed at approximately 286.5 and 288 eV, respectively. Additionally,  $\Pi$ – $\Pi^*$  excitation peaks appear at 290–293 eV.<sup>41</sup> Due to the asymmetry of the graphene XPS spectral peaks, a trailing effect is evident.

#### 4. CONCLUSIONS

In this study, utilizing Puan anthracite as the raw material, we successfully synthesized turbine-layered coal-based graphene in a very short duration (100 ms) using the FJH method. The sample's morphology, structure, and chemical composition were characterized and analyzed under varying flash voltages. The results indicate that AC-FG exhibits a well-defined 2D graphene structure at a flash voltage of 190 V, highlighting the significance of the flash voltage in controlling the synthesis of the coal-based graphene structure within the FJH process. The ease and speed of synthesis, coupled with the high-quality product, underscore the feasibility of producing coal-based graphene (AC-FG) through FJH treatment of anthracite. This approach can transform low-cost coal into high-value graphene materials, offering economic advantages and product benefits, thus holding substantial reference significance.

#### ■ ASSOCIATED CONTENT

##### SI Supporting Information

The Supporting Information is available free of charge at <https://pubs.acs.org/doi/10.1021/acsomega.3c07438>.

Flash Joule heating equipment description; Sai Yin pulse electro-flash reactor; vacuum reaction chamber; tubular reaction unit; importance of coal sample pretreatment; Raman spectra of FJH-prepared products of unpretreated coal samples; morphological and structural characterization results; SEM images of deashing coal and products with different flash voltages with a scale of  $1\mu\text{m}$ ; HR-TEM images of the products treated with

different flash voltages with a scale of 10nm; Raman fitting of the AC-FG(100~170) by Lorentz; and XPS C1 spectrum of the AC-FG treated with different flash voltages (PDF)

#### ■ AUTHOR INFORMATION

##### Corresponding Author

Hongchao Luo – School of Chemical and Materials Engineering, Liupanshui Normal University, Liupanshui 553004 Guizhou Province, China; [orcid.org/0009-0000-9401-489X](https://orcid.org/0009-0000-9401-489X); Email: [luohongchao120@163.com](mailto:luohongchao120@163.com)

##### Author

Xinjuan Liu – School of Environmental and Chemical Engineering, Dalian University, Dalian 116622 Liaoning Province, China

Complete contact information is available at:

<https://pubs.acs.org/doi/10.1021/acsomega.3c07438>

##### Notes

The authors declare no competing financial interest.

#### ■ ACKNOWLEDGMENTS

This work is financially supported by the Liupanshui Normal University Scientific Research and Cultivation Projects (LPSSYLPY202212), the Liupanshui Normal University High-Level Talent Research Start-up Fund (LPSSYKJJ201602), and the Guizhou Provincial Key Laboratory of Coal Clean Utilization (qiankehepingtairencai [2020] 2001).

#### ■ REFERENCES

- (1) Mao, S.; Chen, J. H. Graphene-based electronic biosensors. *J. Mater. Res.* **2017**, *32* (15), 2954–2965.

- (2) Mei, L. Q.; Zhu, S.; Yin, W. Y.; Chen, C. Y.; Nie, G. J.; Gu, Z. J.; Zhao, Y. L. Two-dimensional nanomaterials beyond graphene for antibacterial applications: current progress and future perspectives. *Theranostics* **2020**, *10* (2), 757–781.
- (3) Han, J. H.; Johnson, I.; Chen, M. W. 3D Continuously Porous Graphene for Energy Applications. *Adv. Mater.* **2022**, *34* (15), 29.
- (4) Yao, L. Y.; Chen, A. Q.; Li, L.; Liu, Y. Preparation, properties, applications and outlook of graphene-based materials in biomedical field: a comprehensive review. *J. Biomater. Sci., Polym. Ed.* **2023**, *34* (8), 1121–1156.
- (5) Yang, K.; Feng, L. Z.; Liu, Z. The advancing uses of nano-graphene in drug delivery. *Expert Opin. Drug Delivery* **2015**, *12* (4), 601–612.
- (6) Jiang, C. P.; Zhao, H. Y.; Xiao, H. Y.; Wang, Y.; Liu, L.; Chen, H. J.; Shen, C. Y.; Zhu, H. X.; Liu, Q. Recent advances in graphene-family nanomaterials for effective drug delivery and phototherapy. *Expert Opin. Drug Delivery* **2021**, *18* (1), 119–138.
- (7) Mamba, G.; Gangashe, G.; Moss, L.; Hariganesh, S.; Thakur, S.; Vadivel, S.; Mishra, A. K.; Vilakati, G. D.; Muthuraj, V.; Nkambule, T. T. I. State of the art on the photocatalytic applications of graphene based nanostructures: From elimination of hazardous pollutants to disinfection and fuel generation. *J. Environ. Chem. Eng.* **2020**, *8* (2), 103505.
- (8) Tour, J. M. Top-Down versus Bottom-Up Fabrication of Graphene-Based Electronics. *Chem. Mater.* **2014**, *26* (1), 163–171.
- (9) Gonzalez, V. J.; Rodriguez, A. M.; Leon, V.; Frontinan-Rubio, J.; Fierro, J. L. G.; Duran-Prado, M.; Munoz-Garcia, A. B.; Pavone, M.; Vazquez, E. Sweet graphene: exfoliation of graphite and preparation of glucose-graphene cocrystals through mechanochemical treatments. *Green Chem.* **2018**, *20* (15), 3581–3592.
- (10) Gu, X. G.; Zhao, Y.; Sun, K.; Vieira, C. L. Z.; Jia, Z. J.; Cui, C.; Wang, Z. J.; Walsh, A.; Huang, S. D. Method of ultrasound-assisted liquid-phase exfoliation to prepare graphene. *Ultrason. Sonochem.* **2019**, *58*, 104630.
- (11) Dao, T. D.; Jeong, H. M. Graphene prepared by thermal reduction-exfoliation of graphite oxide: Effect of raw graphite particle size on the properties of graphite oxide and graphene. *Mater. Res. Bull.* **2015**, *70*, 651–657.
- (12) Li, L.; Zhang, D.; Deng, J. P.; Fang, J. F.; Gou, Y. C. Review-Preparation and Application of Graphene-Based Hybrid Materials through Electrochemical Exfoliation. *J. Electrochem. Soc.* **2020**, *167* (8), 086511.
- (13) Wu, J.; Wang, H. F.; Qiu, J.; Zhang, K. F.; Shao, J. W.; Yan, L. F. Efficient preparation of high-quality graphene via anodic and cathodic simultaneous electrochemical exfoliation under the assistance of microwave. *J. Colloid Interface Sci.* **2022**, *608*, 1422–1431.
- (14) Jiang, F.; Yu, Y.; Feng, A. H.; Song, L. X. Effects of ammonia on graphene preparation via microwave assisted intercalation exfoliation method. *Ceram. Int.* **2018**, *44* (11), 12763–12766.
- (15) Li, M.; Yin, B.; Gao, C.; Guo, J.; Zhao, C.; Jia, C.; Guo, X. Graphene: Preparation, tailoring, and modification. In *Exploration*; Wiley Online Library, 2023; Vol. 3, p 20210233.
- (16) Liu, F. N.; Li, P.; An, H.; Peng, P.; McLean, B.; Ding, F. Achievements and Challenges of Graphene Chemical Vapor Deposition Growth. *Adv. Funct. Mater.* **2022**, *32* (42), 20.
- (17) Le Quang, T.; Huder, L.; Lipp Bregolin, F.; Artaud, A.; Okuno, H.; Mollard, N.; Pouget, S.; Lapertot, G.; Jansen, A. G. M.; Lefloch, F.; et al. Epitaxial electrical contact to graphene on SiC. *Carbon* **2017**, *121*, 48–55.
- (18) Islam, F.; Tahmasebi, A.; Moghtaderi, B.; Yu, J. L. Structural Investigation of the Synthesized Few-Layer Graphene from Coal under Microwave. *Nanomaterials* **2022**, *12* (1), 57.
- (19) Luong, D. X.; Bets, K. V.; Algozeeb, W. A.; Stanford, M. G.; Kittrell, C.; Chen, W.; Salvatierra, R. V.; Ren, M. Q.; McHugh, E. A.; Advincula, P. A.; et al. Gram-scale bottom-up flash graphene synthesis. *Nature* **2020**, *577* (7792), 647–651.
- (20) Advincula, P. A.; de Leon, A. C.; Rodier, B. J.; Kwon, J.; Advincula, R. C.; Pentzer, E. B. Accommodating volume change and imparting thermal conductivity by encapsulation of phase change materials in carbon nanoparticles. *J. Mater. Chem. A* **2018**, *6* (6), 2461–2467.
- (21) Hoang, V. C.; Hassan, M.; Gomes, V. G. Coal derived carbon nanomaterials - Recent advances in synthesis and applications. *Appl. Mater. Today* **2018**, *12*, 342–358.
- (22) Huang, P. F.; Zhu, R. T.; Zhang, X. X.; Zhang, W. J. Effect of free radicals and electric field on preparation of coal pitch-derived graphene using flash Joule heating. *Chem. Eng. J.* **2022**, *450*, 137999.
- (23) Inagaki, M.; Kang, F. *Materials Science and Engineering of Carbon: Fundamentals*; Butterworth-Heinemann, 2014.
- (24) Wyss, K. M.; Deng, B.; Tour, J. M. J. N. T. Upcycling and urban mining for nanomaterial synthesis. *Nano Today* **2023**, *49*, 101781.
- (25) Baraniecki, C.; Pinchbeck, P.; Pickering, F. J. C. Some aspects of graphitization induced by iron and ferro-silicon additions. *Carbon* **1969**, *7* (2), 213–224.
- (26) Fiket, Z.; Saikia, B. K.; Chakravarty, S.; Medunić, G. Carbon-based raw materials play key roles in technology of the 21st century: Indian case studies. *Rud. Geol. Naft. Zb.* **2022**, *37* (5), 15–22.
- (27) Sharma, D. K.; Singh, S. K. Advanced process for the production of clean coal by chemical leaching technique. *Energy Sources* **1995**, *17* (4), 485–493.
- (28) Waugh, A.; Bowling, K. M. Removal of mineral matter from bituminous coals by aqueous chemical leaching. *Fuel Process. Technol.* **1984**, *9* (3), 217–233.
- (29) Barma, S. D. Ultrasonic-assisted coal beneficiation: A review. *Ultrason. Sonochem.* **2019**, *50*, 15–35.
- (30) Advincula, P. A.; Luong, D. X.; Chen, W. Y.; Raghuraman, S.; Shahsavari, R.; Tour, J. M. Flash graphene from rubber waste. *Carbon* **2021**, *178*, 649–656.
- (31) Zhang, M.; Chen, K.; Wang, C.; Jian, M.; Yin, Z.; Liu, Z.; Hong, G.; Liu, Z.; Zhang, Y. Mineral-Templated 3D Graphene Architectures for Energy-Efficient Electrodes. *Small* **2018**, *14* (22), 1801009.
- (32) Liao, Y.; Zhu, R.; Zhang, W.; Huang, P.; Sun, Y.; Zhu, H. J. C. Ultrafast synthesis of 3D porous flash graphene and its adsorption properties. *Colloids Surf., A* **2023**, *676*, 132178.
- (33) Wang, L.; Du, C.; Li, Z.; Han, Y.; Feng, N.; Yang, J. Catalytic Graphitization of Coke and Electrochemical Performances of Coke-based Graphite. *J. Alloys Compd.* **2023**, *960*, 170949.
- (34) An, D. M.; Guo, Y. P.; Zhu, Y. C.; Wang, Z. C. A green route to preparation of silica powders with rice husk ash and waste gas. *Chem. Eng. J.* **2010**, *162* (2), 509–514.
- (35) Shcherban, N. D.; Filonenko, S. M.; Yaremov, P. S.; Sergiienko, S. A.; Ilyin, V. G.; Murzin, D. Y. Carbothermal synthesis of porous silicon carbide using mesoporous silicas. *J. Mater. Sci.* **2017**, *52* (7), 3917–3926.
- (36) Wang, X. L.; Yuan, Q. H.; Li, J.; Ding, F. The transition metal surface dependent methane decomposition in graphene chemical vapor deposition growth. *Nanoscale* **2017**, *9* (32), 11584–11589.
- (37) Qin, Y. X.; Li, G. Y.; Gao, Y. P.; Zhang, L. Z.; Ok, Y. S.; An, T. C. Persistent free radicals in carbon-based materials on transformation of refractory organic contaminants (ROCs) in water: A critical review. *Water Res.* **2018**, *137*, 130–143.
- (38) Serrazina, R.; Vilarinho, P. M.; Senos, A.; Pereira, L.; Reaney, I. M.; Dean, J. S. Modelling the particle contact influence on the Joule heating and temperature distribution during FLASH sintering. *J. Eur. Ceram. Soc.* **2020**, *40* (4), 1205–1211.
- (39) Beckham, J. L.; Wyss, K. M.; Xie, Y.; McHugh, E. A.; Li, J. T.; Advincula, P. A.; Chen, W.; Lin, J.; Tour, J. M. Machine learning guided synthesis of flash graphene. *Adv. Mater.* **2022**, *34* (12), 2106506.
- (40) Nan, H. Y.; Ni, Z. H.; Wang, J.; Zafar, Z.; Shi, Z. X.; Wang, Y. Y. The thermal stability of graphene in air investigated by Raman spectroscopy. *J. Raman Spectrosc.* **2013**, *44* (7), 1018–1021.
- (41) Algozeeb, W. A.; Savas, P. E.; Luong, D. X.; Chen, W. Y.; Kittrell, C.; Bhat, M.; Shahsavari, R.; Tour, J. M. Flash Graphene from Plastic Waste. *ACS Nano* **2020**, *14* (11), 15595–15604.